Palaeoenvironmental reconstruction of Northern Spain during the last 8000 cal yr BP based on the biomarker content of the Roñanzas peat bog (Asturias)

José E. Ortiz [a,*], José Luis R. Gallego [b], Trinidad Torres [a], Arantxa Díaz-Bautista [a], Carlos Sierra [b]

[a] *Biomolecular Stratigraphy Laboratory, ETSI Minas, Universidad Politécnica de Madrid, C/Ríos Rosas 21, 28003 Madrid, Spain*
[b] *Environmental Biotechnology and Geochemistry Group, Campus de Mieres, Universidad de Oviedo, C/Gonzalo G, s/n, 33600 Mieres, Asturias, Spain*

A B S T R A C T

We determined the lipid distributions (*n*-alkanes, *n*-methyl ketones, *n*-alkanoic acids, 5-*n*-alkyl resorcinols and sterols) and total organic carbon (TOC) content in a 2.0 m deep *Sphagnum*-dominated ombrotrophic peat bog in Northern Spain. From this, we inferred the changes in plant distribution (*Sphagnum*- vs. non-*Sphagnum*-dominated), which was related to palaeohydrological and palaeoenvironmental conditions, during the last 8000 cal yr BP. From *n*-alkane proxies, 10 dry/humid episodes were distinguished: five dry episodes alternating with five humid episodes, the transitions from dry to humid periods not necessarily being linked to changes in temperature. These transitions were found to correlate well with global environmental episodes and are consistent with other Spanish records. Our results suggest that the *n*-alkane carbon preference index (CPI) could be related to degradation rates linked to variation in temperature rather to changes in the amount of precipitation, whereas the 5-*n*-alkyl resorcinol/sterol ratio could reflect the abundance of sedges.

1. Introduction

Ombrotrophic bogs, characterized by the accumulation of peat in a raised mass over the groundwater table, receive water exclusively from direct precipitation (no input of minerogenic water from the surrounding environment). Therefore, these wetland areas are particularly sensitive to climatic oscillations (Aaby, 1976; Barber, 1985; Barber et al., 1994). The surface wetness of a bog differs, depending on the amount of precipitation and evaporation, and affects the local vegetation biome (Charman, 2002). Furthermore, the high accumulation rate, a characteristic of these mires, and the capacity to preserve organic matter (OM) make ombrotophic bogs exceptional high resolution archives of past climate.

Several techniques have been used to reconstruct palaeoclimate from peat deposits, including macrofossil content (Barber et al., 1994, 2003; Hughes et al., 2006), testate amoebae (Charman, 2001; Hendon et al., 2001; Hughes et al., 2006; Nichols et al., 2006), palynology (Pons and Reille, 1988), humification indices (Blackford and Chambers, 1993) and stable isotopes (White et al., 1994; Figge and White, 1995; Kenny et al., 1999; Ménot and Burns, 2001).

However, where peat humification has destroyed or decayed the macrofossil record, biomarker proxies are particularly relevant (McClymont et al., 2005). Thus, the lipid content of peat bogs provides a valuable record for reconstructing past climate evolution (cf. inter alia del Río et al., 1992; Dehmer, 1993; Lehtonen and Ketola, 1993; Farrimond and Flanagan, 1996; Avsejs et al., 1998; Ficken et al., 1998; Ortiz et al., 2004), even during the Holocene, when relatively subtle climatic shifts occurred (cf. Nott et al., 2000; Avsejs et al., 2002; Xie et al., 2004; McClymont et al., 2005; Zhou et al., 2005; Nichols et al., 2006).

The northwest of the Iberian Peninsula, at mid latitude, provides climatic characteristics of interest. Its oceanic influence is affected by the winter/summer equilibrium of temperate and subtropical components, the latter being responsible for pluviometric seasonality. When linked to areas with an acidic substratum, these climatic conditions allow the development of peat bogs.

For the purpose of this study, we selected the Roñanzas peat bog in Asturias (Fig. 1). Traditionally, peat was extracted by local people for agricultural use and as fossil fuel. In the 1970s and 1980s, it was extracted by a mining company for gardening use. This activity was abandoned in the 1990s, but clean sections in which the sedimentary record crops out are visible.

A previous study indicated that this raised bog was responsive to palaeoenvironmental change. A pollen analysis by Mary et al. (1973), using only 14 samples, noted oscillations in the pollen curves related to palaeoclimatic change. However, according to Desprat et al. (2003) the study of palynological sequences does not provide sufficient temporal resolution for the detection of climatic change at millenial scale and many of the oscillations observed are ambiguously attributed to anthropogenic influence or environmental change (Riera-Mora and Esteban-Amat, 1994; Van der Knaap and Van Leeuwen, 1995; Franco Múgica et al., 1998; Carrión and van Geel, 1999). Thus, we hypothesized that a study

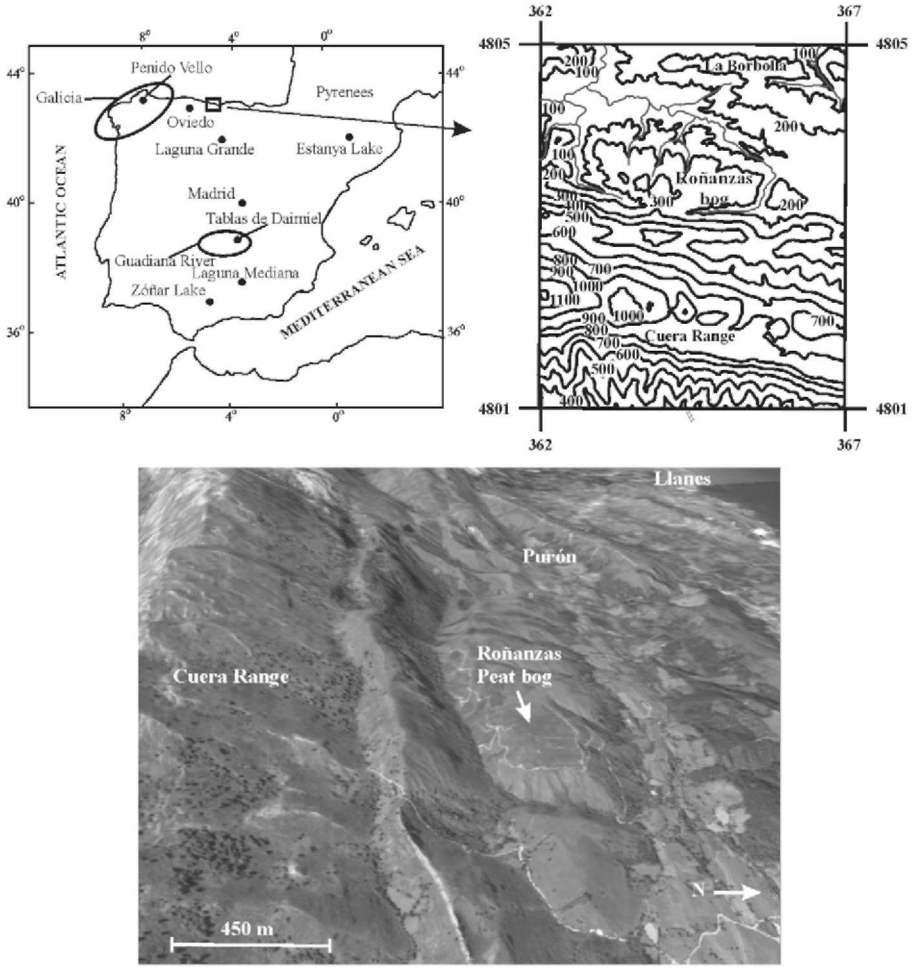

Fig. 1. Geographical and geological setting of Roñanzas peat bog.

of the lipid fraction of the Roñanzas record would provide useful information for the palaeoenvironmental reconstruction of Northern Spain over the last 8 ka cal BP. In fact, Nott et al. (2000) and Nichols et al. (2006) demonstrated that ratios of the abundances of *n*-alkanes provide a new and efficient way of reconstructing past peatlands surface moisture changes, as they found strong correlations among *n*-alkane indices, humification indices and testate amoebae-inferred water table depths of the Minden bog (MI, USA). Avsejs et al. (2002) found that 5-*n*-alkyl resorcinols reflected macrofossil abundances of sedges in a peat profile from Bolton Fell Moss (UK), thereby complementing other data in palaeoclimate studies. Thus, biogeochemical proxies can be used in paleohydrological reconstructions for ombrotrophic bogs to provide a new and complementary source of data from these records.

Moreover, the importance of the Roñanzas peat bog is due to its being one of the scarce bogs in Spain that hold *Sphagnum* species typical of central and northern Europe bogs. In this kind of ombrotrophic mire, certain biomarker proxies have been used to discriminate between *Sphagnum* (moss) vs. *Erica* (heather) predominance and, therefore, between more humid and dryer conditions, respectively (Nott et al., 2000; Pancost et al., 2002; Avsejs et al., 2002; McClymont et al., 2005; Nichols et al., 2006).

2. Geographical and geological setting

Covering ca. 80.000 m^2, the Roñanzas mire is located (43°20′13″N; 04°51′01″W; 250 m) in the eastern part (Llanes County) of the Asturias Province (Northern Spain). It is between 2.0 and 1.5 m in depth and lies on the Ordovician quartzites of the Oville Formation, at the top of one of the several flat surfaces called "rasas" (ancient marine abrasion platforms) that characterize the area (Martínez García, 1980).

The climate is continental with an annual mean temperature of 13.1 °C and annual mean precipitation of 1136 mm/yr (Rivas-Martínez and Rivas y Sáenz, 2006).

The present-day vegetation in the bog includes the following species of moss (Fernández Prieto et al., 1987; Aldasoro et al., 1996): *Sphagnum angustifolium*, *S. capillifolium*, *S. cuspidatum*, *S. denticulatum*, *S. papillosum*, *S. rubellum* and *S. secundum*, together with the following species of algae and vascular plants: *Carex duriaei*, *Drosera intermedia*, *D. rotundifolia*, *Eleocharis palustris*, *Erica mackaiana*, *Eriophorum angustifolium*, *Juncus bulbosus*, *Molinia caerulea*, *Pinguicula grandiflora* and *Rhynchospora alba*.

The presence of the heather *E. mackaiana*, endemic to the North of Spain, must be highlighted because *E. tetralix* is the most common heather in the rest of the world.

Sphagnum mires are not typically located over oligotrophic and impermeable soils, i.e., those of siliceous characteristics, and require flat surfaces. Like other *Sphagnum* mires in the North of Spain, the Roñanzas bog is under a colinous and sub-montanous ecosystem with cool winters and a humid ombroclimate (Fernández Prieto et al., 1987). On the basis of vegetation, climate and physicochemical data, the bog falls within the oceanic intermediate mire cluster (Aldasoro et al., 1996).

We drilled a 2.00 m thick manual core (Fig. 2) in the central part of the bog (20 × 20 cm). We did not observe peat accumulation of

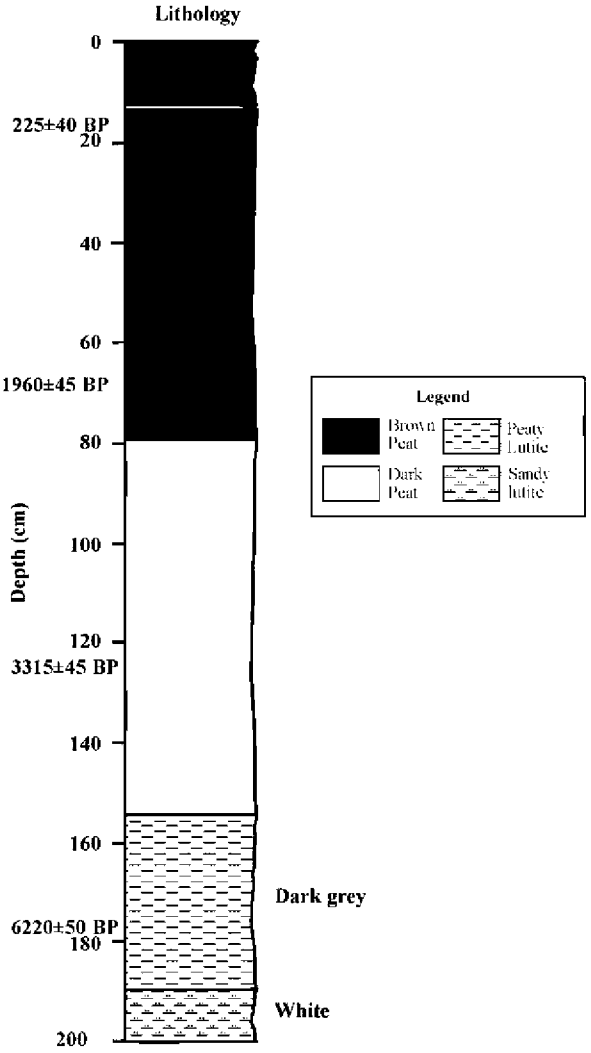

Fig. 2. Stratigraphy and chronology of Roñanzas stratigraphic section. Dates were obtained using the conventional radiocarbon method.

2.5 m (cf. Mary et al., 1973) because the record had suffered compaction as a result of dessication after drainage. In fact, the pollen analysis performed by Mary et al. (1973) was carried out during the first stage of mire exploitation, when it was water saturated. Nevertheless, results obtained here can be compared with those of Mary et al. (1973) because the same zones were distinguished in the lithological record.

We distinguished three clearly distinct zones in the stratigraphic record (Fig. 2): in the lower part, dark-grey lutites with abundant OM were dominant, followed by dark lutitic peat with an oil-like appearance and abundant plant remains, whereas in the uppermost 0.8 m brownish peat predominated with clearly recognisable plant remains. The lowermost 10 cm consisted of white quartzarenites and was not sampled. An interbedded 3 cm thick horizon located at 13 cm with a moss-like texture must be highlighted. We refer to the borehole horizons sampled by depth, in cm, from top to bottom (e.g. sample RO-125 is at 125 cm).

3. Material and methods

The core was split longitudinally in half, photographed and stored frozen at −20 °C until analysis. Samples were taken for conventional radiocarbon dating and lipid analysis.

3.1. Radiocarbon dating

Radiocarbon dating was undertaken on bulk OM of samples taken at 20, 75, 125 and 175 cm at the "Centro Nacional de Aceleradores" (CSIC, Seville, Spain), following pre-treatment with diluted HCl to remove carbonate. The carbon in the samples was reduced to graphite (100%). The graphite was examined for ^{14}C content with an accelerator mass spectrometer, and the radiocarbon age calculated and calibrated using the CALIB 5.0 program (Stuiver and Reimer, 1993; Stuiver et al., 2005).

3.2. TOC concentration

A total of 34 samples (2 g) were taken at 5 cm intervals along the 2.0 m section. They were then homogenized with a mortar and pestle. TOC concentration was measured using a total carbon analyzer (Shimadzu TOC-5000A) equipped with a solid sample module (SSM-5000A). The inorganic carbon fraction had been removed earlier by adding HCl, so the proportional carbon abundance measured (C) was the total organic carbon content (TOC%).

3.3. Lipid extraction and analysis (biomarker analysis)

Another set of 34 samples was used for biomarker analysis. Between 1.3 and 17 g dried sample (at 50 °C for 24 h) were ground and biomarkers were extracted with an accelerated solvent extractor (Dionex ASE 200). Free lipids were extracted with dichloromethane (DCM)/MeOH (2:1) at 1500 psi and 175 °C. The heating phase was 8 min and the static extraction time was 5 min.

The extract was concentrated using a rotary evaporator. Three fractions, A, B and C respectively, were obtained using liquid chromatography with a silica–alumina glass column (14.2 g silica, 7.7 g alumina; 70–230 mm mesh) using solvents of distinct polarity (80 ml in all cases): hexane (A), DCM/hexane 80% (B) and MeOH (C) to yield neutral, polar and acid fractions. Prior to analysis using gas chromatography–mass spectrometry (GC/MS), acidic and polar fractions were methlylated with trimethylsilyldiazomethane and silylated with a mixture of *N,O*-bis(trimethylsilyl)trifluoroacetamide (BSTFA) and pyridine at 70 °C for 2 h. Samples were injected into an HP 6890 gas chromatograph equipped with a selective mass detector (HP 5973) and ATM-5 column (250 × 0.25 mm; 0.20 μm). He was the carrier gas and we used decafluorobiphenyl as an internal standard. The oven temperature was programmed from 60 to 300 °C (held 20 min) at 6 °C/min and the injector was maintained at 275 °C. Components were identified with the Data Analysis program and the Wiley Library; *n*-alkane distributions were obtained from the *m/z* chromatograms (base peak) in fraction A, the *n*-ketones from *m/z* 59 in fraction B, the *n*-alkanoic acids from *m/z* 74 in fraction B, 5-*n*-alkyl resorcinols from *m/z* 268 in fraction C, and sterols and stanols from *m/z* 129 and 215 in fraction C. We only compared amounts of a certain sterol or stanol quantified using the same *m/z* values.

3.4. Biomarker proxies used in peat bogs

3.4.1. n-Alkanes

The *n*-alkane profile in sediments is widely used to discriminate plant origin, i.e., the terrigenous/aquatic input, and is based on the distinct *n*-alkane profiles of algae, aquatic macrophytes and vascular plants. In fact, the hydrocarbon distribution of phytoplankton and algae is dominated by low molecular weight (MW) *n*-alkanes, maximizing at C_{17} (Gelpi et al., 1970; Blumer et al., 1971; Cranwell et al., 1987). Submerged/floating macrophytes maximize at C_{21}, C_{23} and C_{25} (Cranwell, 1984; Ogura et al., 1990; Viso et al., 1993), while emergent macrophytes have *n*-alkane compositions similar to ter-

restrial plants, i.e., peaking at C_{27} and C_{29} (Cranwell, 1984). Terrestrial plants contain high proportions of higher MW *n*-alkanes (C_{27}, C_{29} and C_{31}) in their epicuticular wax (Eglinton and Hamilton, 1963, 1967; Eglinton and Calvin, 1967; Cranwell et al., 1987; Rieley et al., 1991; Nott et al., 2000; Pancost et al., 2002).

More specifically, Baas et al. (2000), Nott et al. (2000), Avsejs et al. (2002), Pancost et al. (2002) and Nichols et al. (2006) recently reported the lipid distributions of various bog-forming plants. On the basis of the *n*-alkane distribution in recent *Sphagnum* and non-*Sphagnum* species typical of bog-forming ecosystems (Baas et al., 2000; Nott et al., 2000; Pancost et al., 2002; Nichols et al., 2006), the predominant *n*-alkane in *Sphagnum* is C_{23}, while *n*-C_{31} is the most abundant in other plants, like in Ericacea (heather, *E. tetralix* and *Calluna vulgaris*) and *Eriophorum* (gramineae), although *C. vulgaris* can also show a maximum at C_{33}. Nevertheless, the profile in some *Sphagnum* species (e.g. *S. capillifolium*, *S. magellanicum*, *S. cuspidatum*) shows a bimodal distribution with a second maximum at C_{31}. *S. papillosum*, *S. palustre* and *S. recurvum* show a unimodal distribution with a maximum at C_{23}.

As the heather *E. mackaiana* is endemic to Northern Spain and is the only Erica species in the Roñanzas peat bog (Fernández Prieto et al., 1987; Aldasoro et al., 1996), we analyzed present day leaves and branches. Similar results were obtained, with a clear predominance of C_{31}, followed by C_{29} and C_{27}.

A number of indices calculated using *n*-alkane abundance are used to better discriminate the origin of OM in peat bog sediments. Thus, the use of the average chain length (ACL), calculated as $[(C_i \times i + C_{i+1} \times (i+1) + C_{i+2} \times (i+2) \cdots + C_n \times n))/(\Sigma C_{n+1} + C_{n+2} + \cdots + C_n)$, with $i = 13$, $n = 33$], was a better proxy for discriminating between the predominance of low vs. high MW *n*-alkanes in Bargerveeen peat bog (The Netherlands; Pancost et al., 2002). Likewise, the variation in C_{23}/C_{31} along a 40 cm peat profile from Bolton Fell Moss (UK) correlated well with changes in vegetation over time, as shown from the macrofossil record (cf. Nott et al., 2000). However, the varying abundance in C_{23} *n*-alkane content should reflect the change in the relative abundance of *Sphagnum* and other high plants and/or variation in *Sphagnum* species.

Consequently, Nichols et al. (2006) preferred to use the C_{23}/C_{29} *n*-alkane ratio to discriminate between major *Sphagnum* vs. other plant inputs, as C_{29} is relatively scarce in *Sphagnum* but abundant in other species, in spite of C_{31} being the most abundant isomer in non-*Sphagnum* plants. However, even this ratio does not represent two pure end members, so they proposed a model correction to the ratio to reduce interference, based on the mean *n*-alkane distribution of *Sphagnum* and non-*Sphagnum* plants. Thus, in the model the portion of C_{23} derived from non-*Sphagnum* species is removed or reduced, as well as the portion of C_{29} belonging to *Sphagnum*. The modelled C_{23}/C_{29} *n*-alkane ratio is indicative of the abundance of *Sphagnum* relative to other plants in peat and is expressed as $[-0.0151(C_{23}/C_{29})^4 + 0.1144(C_{23}/C_{29})^3 - 0.3916(C_{23}/C_{29})^2 + 0.8996(C_{23}/C_{29}) - 0.0455]$.

Ficken et al. (2000) proposed a proxy (*P*aq index), calculated as the $C_{23} + C_{25}/C_{23} + C_{25} + C_{29} + C_{31}$ ratio, to determine the submerged/floating aquatic macrophyte input, which maximizes at the C_{23} and C_{25} *n*-alkanes, relative to the emergent and terrestrial plant input to lake sediments. As the ratio compares the abundance of medium chain *n*-alkanes to the sum of the abundance of medium and long chain *n*-alkanes, and *Sphagnum* species have *n*-alkane profiles similar to those of aquatic macrophytes (cf. Ficken et al., 2000; Baas et al., 2000; Nott et al., 2000; Pancost et al., 2002; Nichols et al., 2006), Nichols et al. (2006) proposed its use for the determination of the relative abundance of *Sphagnum* over other bog-forming plants.

The carbon preference index (CPI) values, calculated as $1/2[(\Sigma C_i + C_{i+2} + \cdots + C_{i+8})/(\Sigma C_{i-1} + C_{i+1} + \cdots + C_{i+7}) + (\Sigma C_i + C_{i+2} + \cdots + C_{i+8})/(\Sigma C_{i+1} + C_{i+3} + \cdots + C_{i+9})]$ ratio, with $i = 25$, were also used by Zheng et al. (2007) to discriminate between palaeoenvironmental conditions, as the *n*-alkanes from the cuticular waxes of higher plants have strong odd/even predominance and give CPI values >5. In contrast, *n*-alkanes from bacteria and algae give low CPI values, around 1 (Cranwell et al., 1987). Because microbial degradation and diagenesis are slowed down during cold and dry conditions (Kuder and Kruge, 1998), CPI values are expected to be high (Xie et al., 2004) and therefore this index could be used for palaeoclimate reconstruction.

3.4.2. *n*-Alkan-2-ones

n-Ketones, in co-operation with *n*-alkanes and other types of organic compounds, provide information about OM sources and its preservation in sediments. Thus, long chain odd numbered *n*-alkan-2-ones between C_{23} and C_{31} are present in all species of *Sphagnum*, maximizing at C_{27}, but are absent from the other most common plant species in ombrothrophic bogs (Morrison and Bick, 1967; Baas et al., 2000; Nichols and Huang, 2007). According to Xie et al. (2004) *n*-alkan-2-ones in the peat of Bolton Fell Moss (Northern England) maximized at either C_{29} or C_{31}.

However, long chain ketones have other possible origins (Arpino et al., 1970; Volkman et al., 1981), including microbial oxidation of the corresponding *n*-alkanes and microbal β-oxidation and decarboxylation of *n*-fatty acids, especially in peat bogs, in which microbial activity can be considerable (cf. Lehtonen and Ketola, 1990; Zheng et al., 2007).

3.4.3. *n*-Alkanoic acids

Like aliphatic hydrocarbons, *n*-alkanoic acids in lake sediments and peat bogs come from OM derived from plants and microorganisms.

Long chain *n*-alkanoic acids (C_{24}–C_{30}), with even predominance are major components of the waxes of land plant leaves, flowers and pollen (Eglinton and Calvin, 1967; Rieley et al., 1991; Meyers and Ishiwatari, 1993) while algae and bacteria maximize at shorter chain lengths, C_{12}–C_{18} (Eglinton and Calvin, 1967; Cranwell et al., 1987).

n-Alkanoic acids in *Sphagnum* are almost exclusively composed of even carbon numbers, with distributions dominated by C_{24} or C_{26} (Baas et al., 2000; Pancost et al., 2002), while in *Erica* C_{30} predominates in roots and leaves and in *Calluna* C_{28} is the most abundant homologue in roots, and C_{24} in leaves and stems (Pancost et al., 2002).

Sometimes diagenetic processes can modify the original *n*-alkanoic acid distribution. Short chain acids are often preferentially degraded by microbes during early diagenesis (Cranwell, 1974, 1976; Haddad et al., 1992; Ho and Meyers, 1994). On the other hand, microbial synthesis of secondary fatty acids from primary organic matter produces short-chain components (Kawamura et al., 1987).

3.4.4. 5-*n*-Alkyl resorcinols and sterols

These components have also been reported to be good palaeoclimatic indicators in mires as they are present solely in distinct proportions in sedges (*Eriophorium*, *Trichophorum* and *Rhynchospora* genus) but not in other plants, such as *Sphagnum* species (Avsejs et al., 2002). In contrast, sterols are typically constituents of *Sphagnum* species, especially stigmasterol and β-sitosterol (Pancost et al., 2002), which are absent from, or present in low concentrations in, other bog-forming plants, with the exception of stigmasterol, abundant in Ericaceae species. Therefore, Xie et al. (2004) used the ratio 5-*n*-alkyl resorcinols/sterols to determine palaeoenvironmental changes.

Table 1
^{14}C dating for sediments from Roñanzas record.[a,b]

Sample	Depth (cm)	Code	$\delta^{13}C$ (‰)	Conventional ^{14}C age (yr BP)	Calibrated age (cal yr BP) 95% Prob.	Calibrated age (yr AD/BC) 95% Prob.
RO-020	20	CNA-319	−27.11	225 ± 40	180 ± 40	1769 ± 40 AD
RO-075	75	CNA-320	−23.65	1960 ± 45	1910 ± 90	40 ± 90 AD
RO-125	125	CNA-321	−26.65	3315 ± 45	3542 ± 100	1583 ± 110 BC
RO-175	175	CNA-322	−26.80	6220 ± 50	7126 ± 130	5177 ± 130 BC

[a] Samples were analyzed using accelerator mass spectrometry (AMS) at Centro Nacional de Aceleradores (Seville, Spain).
[b] Ages calibrated using CALIB 5.0 radiocarbon age calibration program (Stuiver and Reimer, 1993; Stuiver et al., 2005).

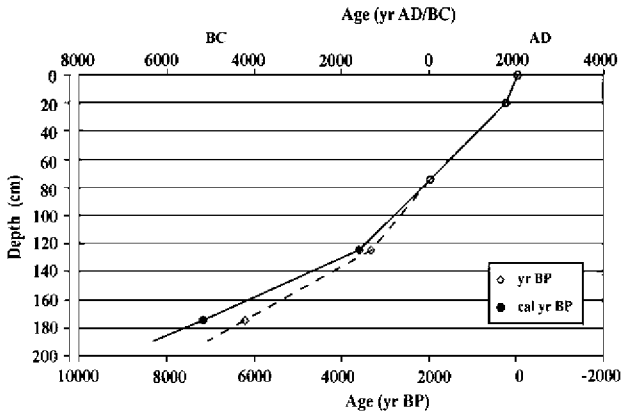

Fig. 3. Age–depth relationship for Padul peat bog core. Dates (Table 1) were obtained using the radiocarbon method.

4. Results

4.1. Chronology

The ages are presented in Table 1 and Fig. 2. The results show that the borehole covers the last 8000 cal yr BP. Fig. 3 shows dating vs. depth, assuming a constant sedimentation between points. This approach allows calculation of the age of undated intermediate horizons, with a chronological scale shown in Fig. 3. The results do not coincide with the radiocarbon ages reported by Mary et al. (1973). In our view, the latter are uncertain because the samples comprised peat from several horizons, some of them with different lithological characteristics (i.e. the intermediate sample ranged from 1.1 to 1.5 m above surface, and the bottom sample from 2.2 to 2.5 m).

4.2. TOC concentration

The concentration of TOC in (Fig. 4) was ca. 1–3% near the bottom, and increased abruptly upwards to between 50% and 60%. From 30 cm to 10 cm, it decreased, with values ranging from 50% to 45%. In the uppermost 10 it returned to previous values.

4.3. Lipids

Distributions of *n*-alkanes, *n*-methyl ketones and *n*-alkanoic acids, together with the relative abundance of 5-*n*-alkyl resorcinols and sterols along the Roñanzas profile are shown in Tables 2 and 3.

4.3.1. n-Alkanes

The logs of the different indices related to the *n*-alkane content, i.e. *n*-alkane predominant chain, average chain length (ACL), *Paq*, C_{23}/C_{31}, C_{23}/C_{29}, modelled C_{23}/C_{29} and CPI, are shown in Figs. 4 and 5.

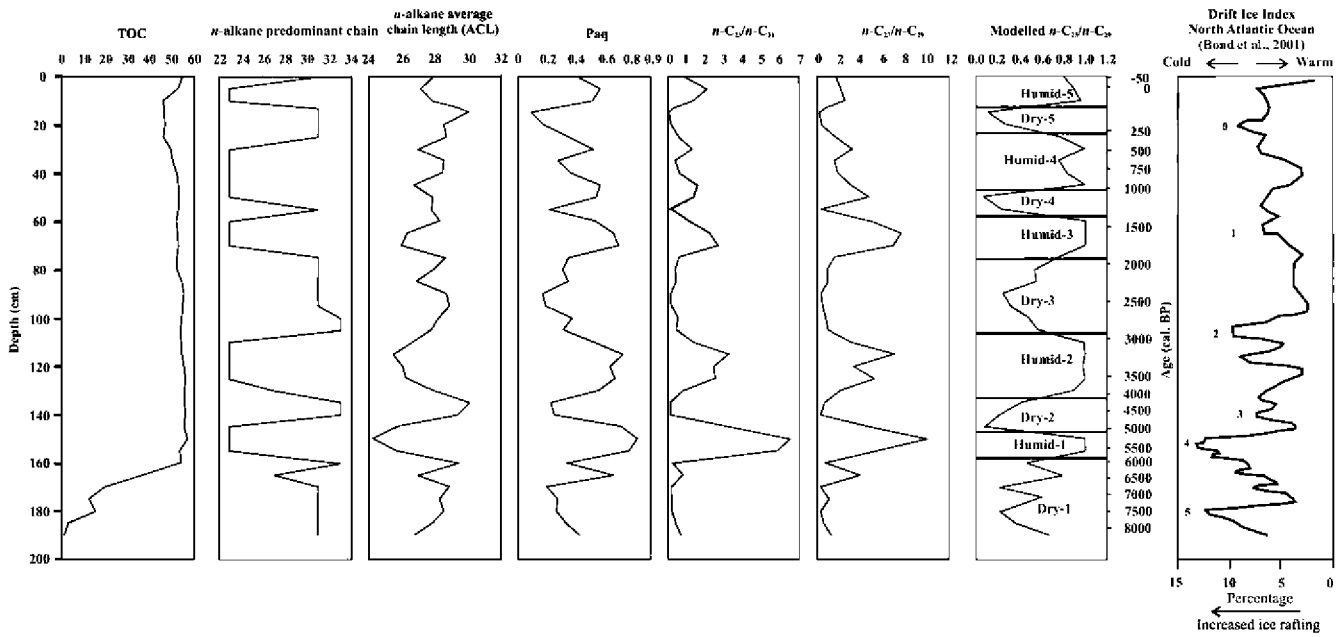

Fig. 4. Profiles of TOC, *n*-alkane predominant carbon number, average chain length (ACL), *Paq* index, C_{23}/C_{31}, C_{23}/C_{29}, modelled C_{23}/C_{29} and CPI. The palaeoenvironmental interpretation is included.

Table 2
Proportion (% of total) of most abundant odd carbon number distributions of *n*-alkanes and *n*-methyl-ketones in Roñanzas record (highest values for each depth in bold).

Depth (cm)	*n*-Alkane C_{no}							*n*-Methyl ketone C_{no}						
	21	23	25	27	29	31	33	17	19	21	23	25	27	29
0	1.62	19.84	4.03	4.61	11.40	**24.07**	17.41	0.13	**64.84**	16.43	3.65	2.84	3.16	2.04
5	0.65	**28.65**	5.99	8.91	13.41	14.02	10.11	0.04	**54.93**	11.51	2.78	3.85	4.86	5.59
10	0.73	**25.52**	4.22	8.38	10.16	19.09	18.09	0.03	**34.16**	7.54	3.07	10.50	14.22	8.90
13	1.54	7.77	4.15	4.85	9.77	**27.83**	25.47	0.13	**24.03**	4.16	4.00	18.93	17.49	8.54
15	2.14	2.04	2.48	4.72	10.67	**35.72**	26.10	0.13	1.09	0.73	3.09	17.47	**24.01**	15.35
20	3.74	4.77	3.66	5.04	11.53	**28.51**	19.72	0.28	8.32	1.63	3.71	15.65	**20.40**	14.25
25	1.00	14.97	3.07	4.12	9.25	**25.59**	21.33	0.01	2.55	1.43	4.91	**26.10**	22.78	8.61
30	2.20	**24.85**	3.80	4.49	7.80	19.47	13.74	0.47	18.80	5.71	4.93	18.47	**20.26**	8.61
35	0.44	15.93	3.52	5.90	10.00	**42.04**	3.20	0.02	**25.44**	6.56	2.75	14.27	21.55	10.79
40	1.51	15.14	3.48	4.58	8.09	**25.70**	21.23	0.15	**24.11**	7.58	3.73	15.49	20.29	10.47
45	1.45	**25.52**	5.37	6.26	8.25	16.18	10.48	0.26	**37.59**	11.60	4.02	11.89	15.22	6.92
50	1.30	**31.68**	2.30	2.56	6.76	23.59	21.58	0.03	**52.86**	13.13	3.26	9.71	10.50	4.38
55	3.57	3.31	5.80	5.76	9.24	**24.09**	19.28	0.30	20.15	5.2	4.75	16.11	**21.86**	12.79
60	1.44	**27.23**	5.71	4.96	5.45	24.04	21.75	0.13	**25.40**	7.85	4.05	11.21	22.30	9.19
65	2.34	**40.25**	3.59	2.59	5.28	18.32	12.43	0.25	**42.70**	10.84	4.52	10.26	12.94	6.56
70	2.47	**37.21**	4.79	4.73	5.36	14.01	11.98	0.34	**39.21**	10.14	4.49	10.99	14.07	8.14
75	2.33	13.78	3.59	3.81	8.74	**24.66**	23.95	0.21	**41.07**	11.00	4.22	9.26	12.56	6.31
80	3.19	8.82	5.20	4.83	9.46	**22.95**	20.87	0.30	**47.71**	10.91	4.11	8.19	11.28	5.41
85	4.51	6.91	5.24	4.34	7.16	**16.39**	15.22	0.25	**37.97**	9.22	4.93	16.10	14.54	4.21
90	2.99	3.93	3.94	4.35	10.21	**28.97**	21.72	0.24	**47.74**	11.44	4.28	9.59	10.51	4.36
95	2.41	5.07	3.84	4.77	10.28	**28.03**	23.97	0.19	**44.04**	9.63	4.51	9.03	10.79	5.67
100	1.74	8.37	7.14	5.59	10.37	16.26	**17.21**	0.16	**33.96**	7.74	4.96	14.12	14.54	6.15
105	3.59	9.13	4.25	4.22	9.14	20.95	**23.02**	0.23	**41.11**	11.65	3.75	9.10	12.44	7.22
110	1.72	**26.49**	3.45	3.81	8.41	19.39	13.19	0.09	**20.76**	6.34	4.34	16.78	18.63	7.07
115	3.06	**37.93**	4.83	4.11	5.42	11.71	9.35	0.16	**27.86**	7.78	4.93	15.09	15.39	6.97
120	3.15	**31.76**	5.94	4.86	9.62	13.04	10.06	0.23	**43.42**	13.83	4.59	10.32	10.85	3.88
125	2.17	**36.04**	5.35	4.43	6.93	14.27	11.88	0.20	**40.40**	11.89	4.00	10.54	11.40	5.91
130	1.45	12.22	14.20	**21.95**	5.70	15.75	17.72	0.16	**28.89**	8.78	3.47	10.02	15.18	9.08
135	1.10	4.17	6.14	2.86	6.19	29.54	**36.57**	0.12	**33.17**	9.18	3.34	9.31	14.76	11.23
140	1.25	3.22	7.67	8.58	9.61	23.47	**27.16**	0.17	**32.97**	7.49	3.45	8.33	12.84	10.87
145	2.58	**35.38**	8.15	4.30	7.57	11.29	10.72	0.21	**53.34**	14.44	4.07	3.87	4.81	6.17
150	18.62	**53.04**	4.71	0.83	5.29	8.13	5.29	0.16	**58.75**	14.18	3.53	3.06	3.78	6.20
155	0.86	**52.10**	3.90	5.21	9.33	8.92	6.58	0.03	**68.48**	12.99	2.43	2.36	2.95	3.07
160	0.00	5.82	8.70	16.06	7.64	21.55	**27.97**	0.13	**22.23**	3.93	1.93	8.00	14.07	12.93
165	1.16	7.85	14.82	**17.73**	2.01	10.15	11.39	0.19	**22.31**	4.86	2.34	8.75	13.27	11.71
170	2.38	4.54	5.14	9.72	13.69	**26.29**	17.34	0.23	**25.90**	6.05	3.71	9.96	10.17	6.82
175	1.98	5.11	7.04	12.45	4.62	**28.54**	16.74	0.26	**30.87**	6.83	4.10	10.66	10.14	6.24
180	1.45	5.03	8.03	13.33	14.46	**22.77**	10.85	0.19	**25.02**	5.57	2.82	8.93	11.48	8.24
185	4.21	7.39	8.04	10.01	12.56	**19.11**	10.71	0.28	**53.97**	11.11	3.46	4.77	5.41	3.89
190	9.44	12.96	7.89	6.73	9.96	**19.14**	11.56	0.35	**62.20**	13.11	3.86	2.88	3.35	2.95

Most of the samples maximized at C_{23} or C_{31} (Fig. 4), suggesting a distinct origin for the OM. In some cases, C_{33} was dominant (RO-100, 105, 135, 140 and 160), which could be linked to the presence of the heather *C. vulgaris* (cf. Pancost et al., 2002), and only in two samples did C_{27} predominate (RO-130 and 165).

Considerable oscillations were observed in the profile of ACL (Fig. 4), i.e. values varied between the marked minimum at 150 cm (24.25) and the maximum located at 135 cm (30.13). The oscillations showed good inverse correspondence with the other indices (*Paq*, C_{23}/C_{31}, C_{23}/C_{29}, and modelled C_{23}/C_{29}).

The *P*aq index values along the Roñanzas section oscillated between 0.1 at 15 cm, and 0.8 at 155 cm, showing a similar profile to the other *n*-alkane ratios, especially the modelled C_{23}/C_{29} one.

The C_{23}/C_{31} ratio also showed several oscillations (Fig. 4), with values >1 and clearly marked maxima at 155–145 cm, 120–110 cm, 70–45 cm and 10–5 cm. Similar oscillations were observed in both the C_{23}/C_{29} and modelled C_{23}/C_{29} *n*-alkane profiles (Fig. 4), i.e. the C_{23}/C_{29} ratio provided maxima (>2) in the same intervals, as well as in the modelled C_{23}/C_{29} ratio.

A sawtooth pattern was apparent in the CPI profile (Fig. 5), oscillating between 2.50 at 100 cm and 10.72 at 50 cm.

4.3.2. n-Alkan-2-ones

The *n*-alkan-2-ones ranged from C_{17} to C_{35}, with a strong odd/even predominance. Almost all the samples showed a bimodal distribution centered around C_{19} and C_{27}.

In general, there was a clear predominance of nonadecan-2-one along all the record (Fig. 5), with the single exception at 55 cm, and between samples at 30 cm and 15 cm, in which heptacosan-2-one was the most abundant homologue, and thus could be attributed to *Sphagnum*-rich horizons.

4.3.3. n-Alkanoic acids

All samples showed a strong even predominance and maximized at C_{24} or C_{26} along the profile, although the sample from 145 cm maximizes at C_{28} (Fig. 5).

4.3.4. 5-n-Alkyl resorcinols and sterols

The 5-*n*-alkyl resorcinols with C_{17}, C_{19}, C_{21}, C_{23} and C_{25} side chains were present at all depths, maximizing at C_{21} and C_{23}. Likewise, there were marked oscillations in the total content of 5-*n*-alkyl resorcinols relative to sample weight (Fig. 5). From the bottom of the section to 140 cm, the lowest abundances were observed, except for RO-170. The pattern changed abruptly in RO-135, which showed a high value. The samples with lower values coincided with the black lutites interval located at the bottom of the section (190–155 cm) and the lowermost part of the peaty interval (from 155 to 140 cm), and did not show any correlation with the *n*-alkane proxies, which showed marked changes in the transition of these intervals. Low abundances were also observed at the top of the section (20–0 cm), whereas between 140 and 20 cm there was a sawtooth pattern, including the marked maximum at 85 cm.

Table 3
Proportion (% of total) of most abundant even *n*-alkanoic acids in Roñanzas record (highest values in bold). Abundances (mg^{-1}) of 5-*n*-alkyl resorcinols and sterols are also shown.

Depth (cm)	*n*-Alkanoic acid C_{no}							5-*n*-Alkyl resorcinols	Sterols
	20	22	24	26	28	30	32		
0	12.13	6.77	**23.97**	21.10	12.28	4.07	1.34	5799719	36292531
5	15.22	4.40	16.71	**19.46**	14.21	5.80	2.79	5518277	9683837
10	13.19	4.43	19.01	21.82	**15.24**	5.77	1.91	4408401	2067935
13	3.70	11.41	**25.44**	16.31	8.85	5.21	2.07	28033836	131742728
15	2.75	9.47	**20.94**	20.29	16.15	4.78	1.41	403470	13155638
20	4.62	11.07	**20.71**	17.09	12.39	5.51	2.60	4703589	35668922
25	1.05	6.95	25.38	**26.92**	18.17	4.25	0.89	21119743	112836302
30	0.76	5.03	23.52	**25.92**	23.03	6.01	1.34	28720869	24902747
35	1.51	9.34	23.53	**31.60**	13.37	4.70	0.68	7671879	58565275
40	0.54	4.28	22.73	**32.98**	22.50	4.77	1.07	72160836	81759151
45	1.01	5.04	24.80	**30.73**	18.87	3.45	0.62	32723022	72543039
50	0.88	7.28	29.21	**29.39**	16.06	3.29	0.84	82470567	73193503
55	2.06	7.19	26.86	**28.36**	17.45	3.85	1.08	4563800	12444508
60	1.36	8.70	24.44	**31.37**	19.03	3.54	0.85	42663833	52867890
65	0.58	8.42	20.88	**40.96**	16.14	3.41	0.80	62092022	65217650
70	2.79	6.68	**28.33**	25.32	14.31	3.61	1.12	43897501	62834733
75	1.44	8.06	27.81	**35.85**	11.56	4.68	1.38	36702301	31054575
80	1.36	7.14	22.25	**35.08**	17.39	4.69	1.39	21426571	37138601
85	0.82	6.04	**32.57**	25.53	16.61	5.07	0.62	136527853	10819093
90	1.88	10.35	**30.66**	26.25	11.74	3.56	1.28	14795635	38621463
95	1.82	11.35	**32.22**	25.77	11.63	3.27	0.90	37481986	43651323
100	1.24	10.36	**30.57**	26.21	14.15	3.68	0.63	43509790	101396348
105	1.20	7.57	25.47	**28.55**	19.13	4.44	0.57	48706210	137839118
110	0.91	7.24	27.39	**28.93**	18.11	4.50	1.01	19245412	60000779
115	1.38	7.23	28.17	**31.62**	16.08	3.33	0.72	44895968	80602145
120	0.96	5.96	22.30	**28.84**	22.09	5.55	0.84	22041972	45249513
125	0.55	4.31	24.66	**34.88**	19.13	4.76	0.52	18307840	29417480
130	1.30	8.32	**32.25**	29.50	15.88	2.60	0.49	5725526	18531353
135	1.20	6.18	**32.20**	27.12	14.12	4.09	1.83	109712047	71843994
140	1.38	11.41	**40.91**	21.54	9.56	2.68	1.02	779693	38011238
145	0.44	3.36	17.67	30.93	**31.88**	5.90	1.39	4150723	27671486
150	2.29	5.93	**30.85**	29.93	12.19	4.70	1.11	7521753	42710515
155	1.95	6.76	**29.76**	22.28	18.30	3.53	1.33	6319712	66380541
160	3.11	7.79	26.28	**26.43**	12.60	4.71	1.81	2528500	15449069
165	6.25	5.45	19.58	**25.34**	13.38	4.93	2.39	737288	8559481
170	3.04	5.32	23.50	**31.15**	15.26	4.33	1.31	4655958	1940021
175	2.21	4.30	22.43	**30.00**	18.12	5.45	1.43	10608990	29875948
180	8.60	4.75	21.37	**28.42**	13.36	5.14	1.55	4942430	85843400
185	5.31	7.98	**24.75**	19.22	15.08	3.35	1.05	536827	7121956
190	3.59	11.98	**29.60**	24.16	9.63	2.85	0.92	231225	3292191

The major sterols and stanols were 24-ethylcholest-5-en-3β-ol (β-sitosterol), 24-ethylcholesta-5,22-dien-3β-ol (stigmasterol), 24-methylcholest-5α-en-3β-ol (campesterol), 24-ethyl-5α-cholestan-3β-ol (stigmastanol), 24-ethyl-5α-cholest-22-en-3β-ol, and 24-methyl-5β-cholestan-3β-ol (campestanol).

The 5-*n*-alkyl resorcinol/sterol ratio (Fig. 5) showed oscillations along the record, with three important maxima at 170, 135 and 10 cm. Lower values were observed, especially at the bottom of the core (190–140 cm) and at 15 cm.

5. Discussion

5.1. TOC concentration

The concentration of TOC is a fundamental proxy for describing OM abundance in sediments (Meyers, 2003). It indicates the OM that escapes remineralization during sedimentation and is influenced by both the initial production of biomass and subsequent degree of degradation, so it integrates OM of distinct origin.

The lower concentration of TOC at the bottom of the record coincides with the point at which detritic sediments are dominant (lutites). The sudden increase from 165 cm marks a dramatic change in the sedimentary record, with a predominance of peaty lutites (between 155 and 80 cm) and peat (from 80 cm to the top).

The correspondence between TOC and lithology can be interpreted in terms of sedimentological characteristics, i.e. the establishment of a bog environment sensu stricto. The high TOC concentration, together with the scarce variation from 165 cm to the top of the core, indicates good OM preservation, as proposed by Meyers and Ishiwatari (1993) and Meyers and Lallier-Verges (1999).

5.2. n-Alkanes

Given the different *n*-alkane profiles of *Sphagnum* (maximizing at C_{23}), *Erica* and other plants (predominance of C_{31} and, in lower proportion, C_{33}), the predominant *n*-alkane chain distribution in the Roñanzas record (Fig. 4) serves as an indicator of changes in vegetation, and therefore of climate conditions. A similar but more accurate interpretation can be made by following the ACL, *Paq* index, C_{23}/C_{31}, C_{23}/C_{29} and modelled C_{23}/C_{29} *n*-alkane ratios. The latter proxy is perhaps the one in which transitions are most clearly defined.

Thus, we identified distinct palaeoenvironmental episodes related to alternating dryer (D) and more humid (H) conditions in the record (Fig. 4), i.e. five main episodes interpreted as humid periods because of the C_{23} *n*-alkane predominance linked to the increase in *Sphagnum*-like species (155–145 cm, 125–110 cm, 70–60 cm, 45–30 cm, 10–5 cm), alternating with another five

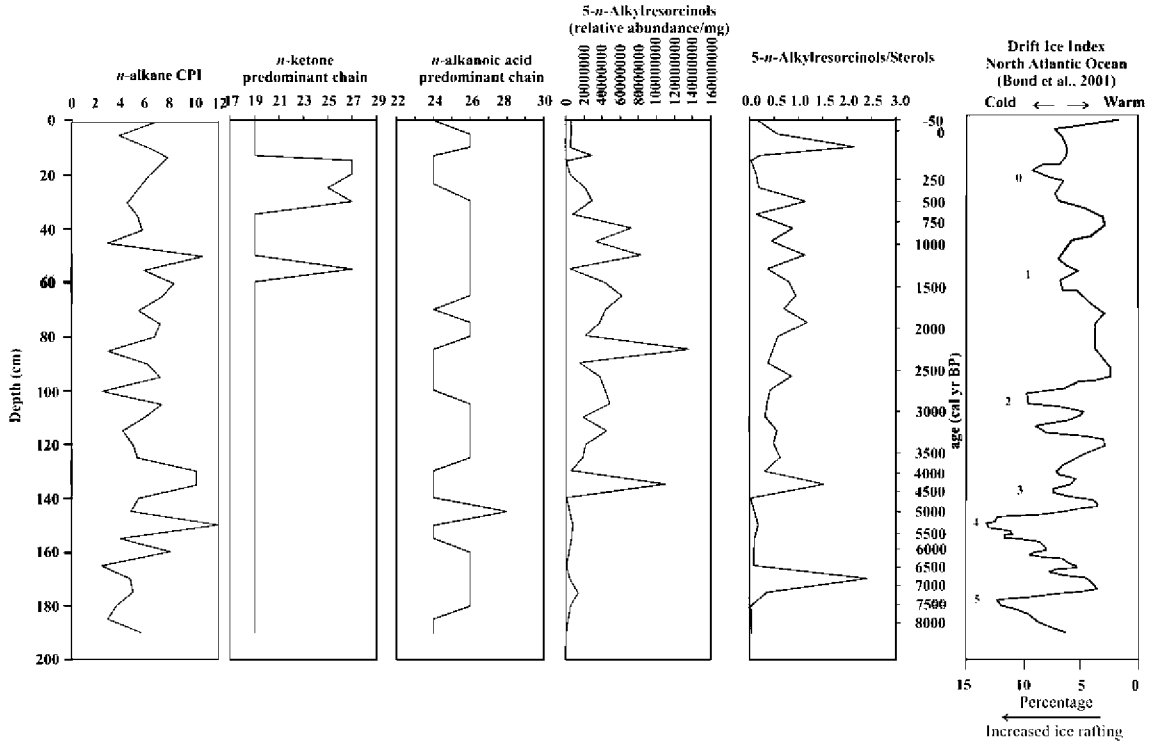

Fig. 5. Records of predominant *n*-methyl ketone chain, predominant *n*-alkanoic acid chain, total content of 5-*n*-alkyl resorcinols (relative abundance mg^{-1}) and 5-*n*-alkyl resorcinol/sterol ratio.

dominated by C_{31} *n*-alkane, linked to the development of Ericacea species (190–160 cm, 140–130 cm, 105–75 cm, 55–50 cm and 25–13 cm) and other plants (140–135 cm, 105–100 cm), which would indicate dryer conditions.

The first dry/humid boundary at 155 cm, dated at ca. 5700 cal yr BP, coincides with the transition from the black lutites, found at the bottom of the stratigraphic section (1.90–1.55 cm), to the peaty interval, which dominates the record (Fig. 4). We propose that this lithological change is linked to palaeoenvironmental shifts, as shown by biomarkers and TOC, when Roñanzas became a peat bog sensu stricto.

The *n*-alkane profiles were compared with the Drift Ice Index for the North Atlantic (Bond et al., 2001), which is related to temperature change (Fig. 4). We observed that the transitions from dry to humid periods are not linked to temperature changes, although in some cases there is a certain correspondence between humid phases and colder periods and dryer episodes with warmer conditions.

Regarding the *n*-alkane CPI values, no correspondence between humid episodes were inferred from the other *n*-alkane proxies and the lowest peaks in the CPI curve, and vice versa (Fig. 5), i.e. there are minima in the CPI profile which coincide with dry periods (e.g. samples at 100, 85 and 45 cm) and maxima that correspond to humid episodes (e.g. samples at 150, 130 and 60 cm). However, in some cases covariation was detected, such as samples 125 and 5, whose low CPI values coincide with humid phases, or the maximum for sample 95, which coincides with a dry phase.

These observations are attributed to the CPI values of *n*-alkanes which could be also related to temperature variation, i.e. the increased CPI value is probably associated with reduced degradation during a cooler period (cf. Xie et al., 2004). This hypothesis is consistent with the proposal by Kuder and Kruge (1998) that lower temperatures are a relevant factor in reducing degradation rates in northern climates. Thus, according Xie et al. (2004) differences in CPI values higher than 2 or 3 in the Bolton Fell Moss profile were enough to interpret cooling or warming events. In fact, the *n*-alkane CPI profile showed certain good correspondence with the Drift Ice Index in the North Atlantic (Bond et al., 2001; Fig. 5), e.g. maxima at 150, 135–130, 105, 60–50 and 15 cm are correlated with the cold Bond Events 4, 3, 2, 1 and 0, respectively.

5.3. n-Alkan-2-ones

The *n*-alkan-2-ones showed a predominance of mainly C_{19}, followed by C_{27} (Fig. 5). The results differ in most cases from those of Baas et al. (2000) and Nichols and Huang (2007), who observed that *Sphagnum* species maximize at C_{27}, whereas in other common plant species in ombrothrophic mires, *n*-alkan-2-ones are absent. Certain plant species that were not included in this study might be responsible for the pattern observed in Roñanzas.

In this regard, the Roñanzas peat bog is unique because the *n*-alkan-2-ones identified by Morrison and Bick (1967) in peat extend over the C_{17}–C_{35} range, with C_{25} and C_{27} being the most abundant homologues. Similarly, Xie et al. (2004) reported a series of *n*-alkan-2-ones in the peat of Bolton Fell Moss in Northern England, which ranged from C_{25} to C_{35}, with a maximum at either C_{29} or C_{31}.

It can be considered that some taxa of bacteria that produce methyl ketones via the metabolism of fatty acids (Lawrence, 1966), fatty alcohols (Hou et al., 1983) and alkanes (Forney and Markovets, 1971), or many taxa of fungi which also produce ketones via an abortive β oxidation sequence (Forney and Markovets, 1971), are responsible for the predominance of the C_{19} ketone. However, fungal or bacterial activity that could produce *n*-methyl ketones with more than 13 carbons is less plausible (Morrison and Bick, 1966; Forney and Markovets, 1971; Fan et al., 1976).

The biodegradation of *n*-alkanes is an alternative explanation for the predominance of C_{19} ketone, especially given that the C_{23} isomer is the most abundant in most *Sphagnum* species. In fact, according to Zheng et al. (2007), microbial activity can be considerable in peat, especially during warm and humid episodes, although Leahy and Colwell (1990) indicated that the characteris-

tics of ombrotrophic bogs (anoxia, low salinity, low nutrient abundance and low pH) are thought to inhibit this activity.

Nevertheless, a similar pattern of *n*-methyl ketone profile to ours from Roñanzas was found by Lehtonen and Ketola (1990). In that study, they ranged from C_{17}–C_{35} but maximized at C_{17}, with the shorter chain C_{17}–C_{23} homologues greatly increasing in abundance with increasing humification. In this regard, *n*-methyl ketones can also be derived from decarboxylation of the even chain length *n*-alkanoic acids in this setting (Arpino et al., 1970; Volkman et al., 1981). In our view, these processes may occur in the Roñanzas bog, in which desiccation produced during peat extraction would have accelerated biodegradation.

5.4. n-Alkanoic acids

Given the observation that all the samples in the profile peaked at C_{24} and C_{26} (Fig. 5) and in *Sphagnum* species C_{24} or C_{26} predominate (Baas et al., 2000; Pancost et al., 2002), and that the C_{24} homologue is also the most abundant in some heather genera (Pancost et al., 2002), we cannot draw any conclusion from the predominant *n*-alkanoic acid chain profile.

5.5. n-Alkyl resorcinols and sterols

The lack of correspondence between the abundance of 5-*n*-alkyl resorcinols and the *n*-alkane proxies (cf. Figs. 4 and 5) could be because these compounds reflect temperature change rather than rainfall, or other processes. In fact, Xie et al. (2004) used the 5-*n*-alkyl resorcinol/sterol ratio to identify warm/cold events, i.e. during cold periods the reduced growth of sedge species produced a decrease in 5-*n*-alkyl resorcinols (Avsejs et al., 2002).

In any case, the distribution of sterols and stanols in the Roñanzas bog is consistent with the dominance of higher plants in the peat, especially of *Sphagnum*-derived origin. In fact, according to Pancost et al. (2002), the C_{29} sterols, stigmasterol (24-ethylcolesta-5,22-dien-3β-ol) and β-sitosterol (24-ethylcholest-5-en-3β-ol), are dominant in *Sphagnum*, although in some species the presence of the C_{28} sterol, campesterol (24-methylcholest-5-en-3β-ol), is also considerable. In contrast, these C_{29} isomers are absent from, or present in very low concentrations in, Ericacea, with the exception of stigmasterol, which is much more abundant in these species.

However, we did not find any clear correlation between the 5-*n*-alkyl resorcinol/sterol ratio and the *n*-alkane CPI and the temperature reconstruction described by Bond et al. (2001) (Fig. 5), i.e. only the cold Bond Events 3 and 1 coincide with increases in the 5-*n*-alkyl resorcinol/sterol ratio. In contrast, we detected an important peak in the ratio at ca. 6800 cal yr BP, which correlates with a warming phase (cf. Bond et al., 2001 – Fig. 5) and the Bond Events 5, 4 and 2 do not appear to have any correspondence in the Roñanzas record. This can be explained because the abundance of stigmasterol, which is considered in the total content of sterols, is

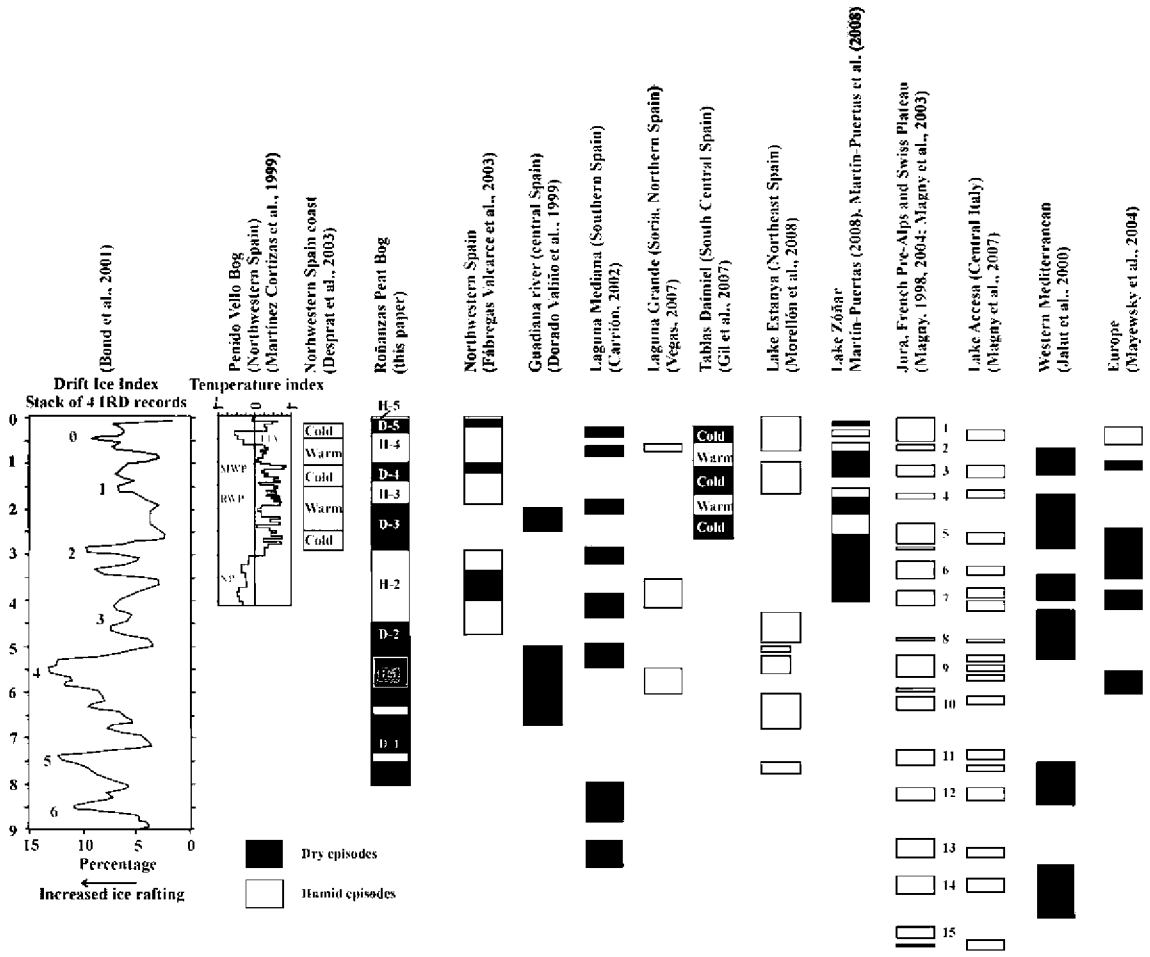

Fig. 6. Comparison of palaeoenvironmental periods established for the Roñanzas bog with other records for Spain and other regions of Europe. The temperature reconstruction for the last 4 ka BP by Martínez Cortizas et al. (1999), inferred from the Hg content of a peat bog in northwestern Spain, is included, together with the percentage Drift Ice Index for the North Atlantic during the last 9 ka BP (cf. Bond et al., 2001). IRD, ice rafted debris; NP, Neoglacial Period; RWP: Roman Warm Period; MWP: Medieval Warm Period; LIA: Little Ice Age. Site location in Spain is shown in Fig. 1.

present both in *Sphagnum* and Ericacea species, which are related to distinct rainfall conditions and can be present either in humid or dry phases.

Thus, we propose that the total content of 5-*n*-alkyl resorcinols in Roñanzas is related mainly to the abundance of sedges (*Eriophorium*, *Trichophorum* and *Rhynchospora* genus) and not directly to temperature or rainfall.

5.6. Palaeoenvironmental considerations

We compared the inferred palaeoprecipitation record (Fig. 6) with the Drift Ice Index for the North Atlantic during the last 9 ka BP (cf. Bond et al., 2001), which is related to temperature variation, and with the temperature reconstruction for the last 4 ka BP, inferred from the Hg content of a peat bog in Northwestern Spain (Martínez Cortizas et al., 1999). We also correlated the humid and dry episodes with other European records (Fig. 6).

The bottom of the Roñanzas record (8000–5900 cal BP), which is correlated with the Atlantic Period, is characterized by variability in rainfall, also observed by Kaplan and Wolfe (2006) for the North Atlantic region. Nevertheless, in Roñanzas there is a general trend towards less precipitation (1st Dry Period – Fig. 4), which coincides with the palynological review studies of Salas (1992) and González-Díez et al. (1996) relating to the pollen record of different Northern Spain records. Similarly, a good correspondence is observed with Vegas (2007) and Jalut et al. (2000) (Fig. 6).

This episode coincides with the Mesolithic/Neolithic transition in Northern Spain at 6000–5500 cal yr BP, which was marked by ancient human groups moving away from hunting/gathering activities towards mainly agriculture/pastoral activities (Arias, 1999; Peña-Chocarro et al., 2005) or probably slightly earlier (cf. González-Morales, 1982, 1992). This process of "domesticating" the landscape, which produced deforestation and the presence of clearings (Martínez Cortizas et al., 2009), is evidenced in archaeological sequences by a decrease in arboreal pollen, accompanied by a similar increase in thickets, bushes and cereals, especially emmer wheat and einkorn (Peña-Chocarro et al., 2005) in peat bog records like Los Tornos (Peñalba, 1989; Muñoz Sobrino, 2001) and others in Galicia (Northwestern Spain) (Martínez Cortizas et al., 2009). Likewise, Mary et al. (1973) found low proportions of *Corylus* and a higher content of *Poeacea* and *Compositae* pollen, together with cereal grains, at the bottom of the Roñanzas record.

Nevertheless, two phases of wetter conditions are observed within this 1st Dry Period. These show good correspondence with phases of higher lake levels in European water bodies (Magny, 1998, 2004; Magny et al., 2003, 2007; Fig. 6).

The increase in rainfall during the following episode (1st Humid Period; 5900–5200 cal yr BP – Fig. 4), also observed by Magny (1998, 2004), Reed et al. (2001), Magny et al. (2003, 2007) and Vegas (2007) in European records (Fig. 6), marks the Atlantic/Subboreal transition and is accompanied by a temperature decrease coinciding with the Bond Event 4 (cf. Bond et al., 2001; Fábregas Valcarce et al., 2003; Fig. 6).

The 2nd Dry Period (5200–4200 cal yr BP) is correlated with a dry phase observed for Southern Spain (Carrión, 2002), some Galician bogs (Fábregas Valcarce et al., 2003) and the Mediterranean coast of Spain and Southern France (Jalut et al., 2000) (Fig. 6).

The onset of the 2nd Dry Period corresponded with a marked decrease in ice rafted debris (IRD) in the North Atlantic, although the end coincides with Bond Event 3 (Bond et al., 2001; Fig. 6).

The 2nd Humid Period (4200–2900 cal yr BP – Fig. 4) is correlated with high lake-level episodes in Europe (Magny, 1998, 2004; Magny et al., 2003, 2007; Fábregas Valcarce et al., 2003; Vegas, 2007) and the increase in humidity in the Southestern Mediterranean basin (Schilman et al., 2001). However, these humid conditions do not coincide with some other areas, in which dry conditions were described, i.e. Mediterranean region (Jalut et al., 2000), Pyrenees (Morellón et al., 2008), Southern Spain (Martín-Puertas et al., 2008) and at a global scale (Mayewski et al., 2004).

Temperature varied along this humid episode: at the beginning temperate conditions occurred, while in the middle, warmer temperatures were interpreted (lower IRD index), finishing with colder temperatures coinciding with Bond Event 2 (Bond et al., 2001).

The 3rd Dry Period (2900–1900 cal yr BP – Fig. 4) coincides with dry phases observed in the Mediterranean region (Roca and Julià, 1997; Harrison et al., 1999; Dorado-Valiño et al., 1999; Jalut et al., 2000; Carrión, 2002; Gil-García et al., 2007), Northern Africa (Lamb et al., 1999, 2004; Lamb, 2001) and Northern Spain (González-Sampériz and Sopena Vicién, 2002; Leira, 2005; González-Sampériz et al., 2008; Fig. 6). However, according to Magny (1998, 2004) and Magny et al. (2003), a general high lake-level episode is observed for European water bodies at 2750–2350 cal yr BP (Fig. 6).

The rafted debris index record for the North Atlantic indicates warm conditions (except at the beginning) and, similarly, according to Martínez Cortizas et al. (2009), many indicators show an acceleration in environmental degradation as a result of human activities from 1.5 to 1 ka cal BC (2.5–2.0 cal yr BP; Fig. 6).

The beginning of the 3rd Humid Period in the Roñanzas record (1900–1200 cal yr BP, 50–750 AD – Fig. 4) coincides with the beginning of the Roman Period. The end of the 3rd Humid Period corresponds to the cold period of the Dark Ages (cf. Martínez Cortizas et al., 1999; Desprat et al., 2003) and the cold Event 1 of Bond et al. (2001), coinciding also with the decrease in temperature observed in some records (Muller and MacDonald, 2000; Desprat et al., 2003) and interpreted from the Hg content in a Northwestern Iberian peat bog record, which preludes the onset of the Medieval Warm Period (Martínez Cortizas et al., 1999; Fig. 6).

Increasing moisture during the Roman Period and the Dark Ages has also been reported in Southern Spain (Gil-García et al., 2007; Martín-Puertas et al., 2008), other Iberian records (González-Sampériz and Sopena Vicién, 2002; Desprat et al., 2003; González-Sampériz et al., 2008; Morellón et al., 2008), Africa (Lamb et al., 1999, 2004), Israel (Schilman et al., 2001) and central Europe (Magny, 1998, 2004; Magny et al., 2003, 2007) (Fig. 6).

During the Medieval Optimum (ca. 1200–600 cal yr BP, 750–1350 AD), characterized by a global progressive increase in temperature, not only in Northwestern Spain (Martínez Cortizas et al., 1999; Desprat et al., 2003) but also in North Atlantic latitudes (Muller and MacDonald, 2000; Bond et al., 2001), rainfall diminished in the Roñanzas area (4th Dry Period, 1200–830 cal yr BP, 750–1100 AD – Fig. 4). This decrease is also reflected in other records from Northwestern Iberia (Desprat et al., 2003), central Spain (Juliá et al., 1998; Valero Garcés et al., 2008), Southern Spain (Gil-García et al., 2007) the Pre-Pyrenean Range (Riera et al., 2004; Morellón et al., 2008), Southern and Central Europe (Magny, 1998, 2004; Jalut et al., 2000; Magny et al., 2003, 2007), Africa (Johnson et al., 1991; Lamb et al., 1999, 2004), Israel (Bar-Matthews et al., 1999), and globally (Mayewski et al., 2009; Fig. 6).

The 4th Dry Period can be correlated with low water level phases in lakes from the Spanish Pyrenees (Riera et al., 2004) and Southern Spain (Martín-Puertas et al., 2008).

The 4th Humid Period (ca. 830–230 cal yr BP AD – Fig. 4) marks the transition from the Medieval Optimum to the Little Ice Age (ca. 1200–1650 AD; 750–300 yr cal BP), characterized by colder conditions and increased rainfall in Mediterranean areas (Issar, 2003), especially central Northern Spain (Desprat et al., 2003; Riera et al., 2004; Gil-García et al., 2007; Vegas, 2007; Morellón et al., 2008) (Fig. 6). Furthermore, according to Jalut et al. (2000), Issar (2003), Magny (1998, 2004), Magny et al. (2003, 2007) and Mayewski et al. (2004) a more humid climate occurred in central Europe, in the Eastern Mediterranean (Bar-Matthews et al., 1999) and Africa (Roberts et al., 1994; Lamb et al., 1999; Verschuren et al., 2000).

The 5th Dry Period (230–80 yr cal BP – Fig. 4) corresponds to the maximum onset of the Little Ice Age (300–100 yr cal BP), characterized by high climate variability but under lower temperatures, as observed for Northwestern Spain (Martínez Cortizas et al., 1999), the North Atlantic (Event 0 of Bond et al., 2001) and worldwide, with glacier advance (Magny, 1998; Magny et al., 2002). In fact, Martín Vide and Olcina Cantos (2001) indicate that four catastrophic episodes are documented in Spain from the second half of the 15th century to the 19th century, in which intensive precipitation, snowfall and thunderstorms were common, alternating with severe droughts, as recorded in other localities from Southern and Northern Spain (Riera et al., 2004; Gil-García et al., 2008; Martín-Puertas et al., 2008; Fig. 6).

The 5th Humid Period (80 to –20 cal yr BP – Fig. 4) corresponds to the 20th century, in which increasing rainfall is interpreted to occur. Nevertheless, we detected a progressive decrease in humidity at the top of Roñanzas record.

6. Conclusions

The deposition and preservation of peat in the Roñanzas ombrotrophic mire in Northern Spain have been controlled mainly by rainfall, as shown by the lipid biomarker proxies and the TOC in the 2.0 m deep record. The *n*-alkane proxies (predominant carbon number, average chain length, P*aq* index, C_{23}/C_{31}, C_{23}/C_{29}, modelled C_{23}/C_{29} ratio) show considerable variation, interpreted in terms of vegetation changes (*Sphagnum* vs. non-*Sphagnum*-dominated phases) along the last 8000 cal yr BP and therefore related to precipitation. Thus, we defined five Dry Episodes alternating with five Humid Episodes. However, the transitions from dry to humid periods are not linked to temperature change, as observed when comparing these periods with the temperature reconstruction of Martínez Cortizas et al. (1999), Muller and MacDonald (2000) and Bond et al. (2001). Nevertheless, the episodes show good correspondence with global and other Spanish records. Furthermore, the *n*-alkane CPI seems to be related to degradation rates influenced by temperature oscillations, while the 5-*n*-alkyl resorcinol/sterol ratio appears to reflect the abundance of sedges.

Acknowledgements

This research was an internal project LEB-3-2007 of the Biomolecular Stratigraphy Laboratory of the Madrid School of Mines. The Biomolecular Stratigraphy Laboratory has been partially funded by ENRESA and the Spanish Geological Survey (Instituto Geológico y Minero de España). We thank B. Jansen and an anonymous reviewer for helpful comments.

Associate Editor—**K.G.J. Nierop**

References

Aaby, B., 1976. Cyclic climatic variations in climate over the past 5500 years reflected in raised bogs. Nature 263, 281–284.

Aldasoro, J.J., Aedo, C., Muñoz, J., de Hoyos, C., Vega, J.C., Negro, A., Moreno, G., 1996. A survey on Cantabrian mires (Spain). Anales del Jardín Botánico de Madrid 54, 472–489.

Arias, P., 1999. The origins of the Neolithic along the Atlantic coast of Continental Europe: a survey. Journal of World Prehistory 13, 403–464.

Arpino, P., Albrecht, P., Ourisson, G., 1970. Series homologues aliphatics dans un sediment Eocène d'origen lacustre. Comptes Rendus Academie de Science, Series D 270, 1760–1763.

Avsejs, L.A., Nott, C.J., Maxwell, J.R., Evershed, R.P., 1998. Hydroxy and ketonic androstanes: a new class of sterol diagenetic product in peat. Organic Geochemistry 28, 749–753.

Avsejs, L.A., Nott, C.J., Xie, S., Maddy, D., Chambers, F.M., Evershed, R.P., 2002. 5-*n*-Alkylresorcinols as biomarkers of sedges in an ombotrophic peat section. Organic Geochemistry 33, 861–867.

Baas, M., Pancost, R., van Geel, B., Sinninghe Damsté, J.S., 2000. A comparative study of lipids in *Sphagnum* species. Organic Geochemistry 31, 535–541.

Barber, K.E., 1985. Peat stratigraphy and climatic changes: some speculations. In: Tooley, M.J., Sheail, G.M. (Eds.), The Climatic Scene: Essays in Honour of Gordon Manley. Allen and Unwin, London, pp. 175–185.

Barber, K.E., Chambers, F.M., Maddy, D., Stoneman, R., Brew, J.S., 1994. A sensitive high resolution record of late Holocene climatic change from a raised bog in northern England. The Holocene 4, 198–205.

Barber, K.E., Chambers, F.M., Maddy, D., 2003. Holocene palaeoclimates from peat stratigraphy: macrofossil proxy climate records from three oceanic raised bogs in England and Ireland. Quaternary Science Reviews 22, 521–539.

Bar-Matthews, M., Ayalon, A., Kaufman, A., Wasserburg, G.J., 1999. The Eastern Mediterranean paleoclimate as a reflection of regional events: Soreq cave Israel. Earth and Planetary Science Letters 166, 85–95.

Blackford, J.J., Chambers, F.M., 1993. Determining the degree of peat decomposition in peat-based palaeoclimatic studies. International Peat Journal 5, 7–24.

Blumer, M., Guillard, R.R.L., Chase, T., 1971. Hydrocarbons of marine plankton. Marine Biology 8, 183–189.

Bond, G., Kromer, B., Beer, J., Muscheler, R., Evans, M.N., Showers, W., Hoffmann, S., Lotti-Bond, R., Hajdas, I., Bonani, G., 2001. Persistent solar influence on North Atlantic climate during the Holocene. Science 278, 1257–1266.

Carrión, J.S., 2002. Patterns and processes of late Quaternary environmental change in a montane region of southwestern Europe. Quaternary Science Reviews 2, 2047–2066.

Carrión, J.S., van Geel, B., 1999. Palaeocological evidence of pollen sequence in eastern Spain: challenges existing concepts of vegetation change. South African Journal of Science 95, 44–46.

Charman, D.J., 2001. Biostratigraphic and palaeoenvironmental applications of testae amoebae. Quaternary Science Reviews 20, 1753–1764.

Charman, D.J., 2002. Peatlands and Environmental Change. John Wiley and Sons, West Sussex.

Cranwell, P.A., 1974. Monocarboxilic acids in lake sediments: indicators, derived from terrestrial and aquatic biota, of paleoenvironmental trophic levels. Chemical Geology 14, 1–14.

Cranwell, P.A., 1976. Decomposition of aquatic biota and sediment formation: lipid components of 2 blue-green algal species and of detritus resulting from microbial attack. Freshwater Biology 6, 481–488.

Cranwell, P.A., 1984. Lipid geochemistry of sediments from Upton Broad, a small productive lake. Organic Geochemistry 7, 25–37.

Cranwell, P.A., Eglinton, G., Robinson, N., 1987. Lipids of aquatic organisms as potential contributors to lacustrine sediments-II. Organic Geochemistry 11, 513–527.

Dehmer, J., 1993. Petrological and organic geochemical investigation of recent peats with known environments of deposition. International Journal of Coal Geology 28, 111–138.

del Río, J.C., Gónzalez-Vila, F.J., Martin, F., 1992. Variation in the content and distribution of biomarkers in two closely situated peat and lignite deposits. Organic Geochemistry 18, 67–78.

Desprat, S., Sánchez Goñi, M.F., Loutre, M.F., 2003. Revealing climatic variability of the last three millennia in northwestern Iberia using pollen influx data. Earth and Planetary Science Letters 213, 63–78.

Dorado Valiño, M., Valdeolmillos Rodríguez, A., Ruiz Zapata, B., de Bustamante Gutiérrez, I., 1999. Evolución climática durante el Holoceno en la cuenca alta del Guadiana (Submeseta sur Ibérica). Cuaternario y Geomorfología 13, 19–32.

Eglinton, G., Calvin, M., 1967. Chemical fossils. Scientific American 216, 32–43.

Eglinton, G., Hamilton, R.J., 1963. The distribution of *n*-alkanes. In: Swain, T. (Ed.), Chemical Plant Taxonomy. Academic Press, London, pp. 87–217.

Eglinton, G., Hamilton, R.J., 1967. Leaf epicuticular waxes. Science 156, 1322–1335.

Fábregas Valcarce, R., Martínez Cortizas, A., Blanco Chao, R., Chesworthd, W., 2003. Environmental change and social dynamics in the second–third millennium BC in NW Iberia. Journal of Archaeological Science 30, 859–871.

Fan, T.Y., Hwang, D.H., Kinsella, JE., 1976. Methyl ketone formation during germination of *Penicillium roqueforti*. Journal of Agricultural and Food Chemistry 24, 443–448.

Farrimond, P.F., Flanagan, R.L., 1996. Lipid stratigraphy of a Flandrian peat bed (Northumberland, UK): comparison with the pollen record. The Holocene 6, 69–74.

Fernández Prieto, J.A., Fernández Ordóñez, M.C., Collado Prieto, M.A., 1987. Datos sobre la vegetación de las «turberas de esfagnos» galaico-asturianas y orocantábricas. Lazaroa 7, 443–471.

Ficken, K.J., Barber, K.E., Eglinton, G., 1998. Lipid biomarker, $\delta^{13}C$ and plant macrofossil stratigraphy of a Scottish montane peat bog over the last two millennia. Organic Geochemistry 28, 217–237.

Ficken, K.J., Li, B., Swain, D.L., Eglinton, G., 2000. An *n*-alkane proxy for the sedimentary input of submerged/floating freshwater aquatic macrophytes. Organic Geochemistry 31, 745–749.

Figge, R.A., White, J.W.C., 1995. High-resolution Holocene and late glacial atmospheric CO_2 record: variability tied to changes in thermohaline circulation. Global Biogeochemical Cycle 9, 391–403.

Forney, F.W., Markovets, A.J., 1971. The biology of methyl ketones. Journal of Lipid Research 12, 383–395.

Franco Múgica, F., García Antón, M., Sainz Ollero, H., 1998. Vegetation dynamics and human impact in the Sierra de Guadarrama, Central System, Spain. The Holocene 8, 69–82.

Gelpi, E., Scheider, H., Mann, J., Oro, J., 1970. Hydrocarbons of geochemical significance in microscopic algae. Phytochemistry 9, 603–612.

Gil-García, M.J., Ruiz Zapata, M.B., Santisteban, J.I., Mediavilla, R., López Pamo, E., Dabrio, C.J., 2007. Late Holocene environments in las Tablas de Daimiel (south central Iberian Peninsula, Spain). Vegetation History and Archaeobotany 16, 241–250.

Gil-García, M.J., Ruiz Zapata, M.B., Mediavilla, R., Santisteban, J.I., Domínguez-Castro, F., Dabrio, C.J., 2008. Registro de los cambios humanos y naturales en el humedal de las Tablas de Daimiel (Ciudad Real, España). Geo-Temas 10, 1471–1474.

González-Díez, A., Salas, L., Díaz de Terán, J.R., Cendrero, A., 1996. Late Quaternary climate changes and mass movement frequency and magnitude in the Cantabrian region, Spain. Geomorphology 15, 291–309.

González-Morales, M.R., 1982. El Asturiense y otras Culturas Locales. Monografías del Centro de Investigación y Museo de Altamira, Santander.

González-Morales, MR., 1992. Mesolíticos y Megalíticos: la evidencia arqueológica de los cambios en las formas productivas en el paso al megalitismo en la costa cantábrica. In: Moure, A. (Ed.), Elefantes, Ciervos y Ovicaprinos: Economía y Aprovechamiento del Medio en la Prehistoria de España y Portugal. Universidad de Cantabria, Santander, pp. 185–202.

González-Sampériz, P., Sopena Vicién, M.C., 2002. Recent Holocene palaeoenvironmental evolution in the central Ebro Basin (NE Spain). Quaternary International, 177–190.

González-Sampériz, P., Valero-Garcés, B.L., Moreno, A., Morellón, M., Navas, A., Machín, J., Delgado-Huertas, A., 2008. Vegetation changes and hydrological fluctuations in the Central Ebro Basin (NE Spain) since the late glacial period: saline lake records. Palaeogeography, Palaeoclimatology, Palaeoecology 259, 157–181.

Haddad, R.I., Martens, C.S., Farrington, J.W., 1992. Quantifying early diagenesis of fatty acids in rapidly accumulating coastal marine sediments. Organic Geochemistry 19, 205–216.

Harrison, S.P., Jolly, D., Laarif, F., Abe-Ouchi, A., Dong, B., Herterich, K., Hewitt, C., Joussaume, S., Kutzbach, J.E., Mitchell, J., De Noblet, N., Valdes, P., 1999. Intercomparison of simulated global vegetation distributions in response to 6 kyr BP orbital forcing. Journal of Climate 11, 2721–2742.

Hendon, D., Charman, D.J., Kent, M., 2001. Palaeohydrological records derived from testae amoebae analysis from peatlands in northern England: within-site variability, between-site comparability and palaeoclimatic implications. The Holocene 11, 127–148.

Ho, E.S., Meyers, P.A., 1994. Variability of early diagenesis in lake sediments: evidence from the sedimentary geolipid record in an isolated tarn. Chemical Geology 112, 309–324.

Hou, C.T., Patel, R., Laskin, A.I., Barnabe, N., Barist, I., 1983. Production of methyl ketones from secondary alcohols by cell suspensions of C_2 to C_4 *n*-alkane-grown bacteria. Applied and Environmental Microbiology 46, 178–184.

Hughes, P.D.M., Blundell, A., Charman, D.J., Bartlett, S., Daniell, J.R.G., Wojatschke, A., Chambers, F.M., 2006. An 8500 cal. year multi-proxy climate record from a bog in eastern Newfoundland: contributions of meltwater discharge and solar forcing. Quaternary Science Reviews 25, 1208–1227.

Issar, A.S., 2003. Climate Changes during the Holocene and Their Impact on Hydrological System. Cambridge University Press, Cambridge, UK.

Jalut, G., Amat, A.E., Bonnet, L., Gauquelin, T., Fontugne, M., 2000. Holocene climatic changes in the Western Mediterranean, from south-east France to south-east Spain. Palaeogeography, Palaeoclimatology, Palaeoecology 160, 255–290.

Johnson, T.C., Halfman, J.D., Showers, W.J., 1991. Paleoclimate of the past 4000 years at Lake Turkana, Kenya, based on the isotopic composition of authigenic calcite. Palaeogeography, Palaeoclimatology, Palaeoecology 85, 189–198.

Juliá, R., Burjachs, F., Dasí, M.J., Mezquita, F., Miracle, M.R., Roca, J.R., Seret, G., Vicente, E., 1998. Meromixis origin and recent trophic evolution in the Spanish mountain lake La Cruz. Aquatic Sciences 60, 279–299.

Kaplan, M.R., Wolfe, A.P., 2006. Spatial and temporal variability of Holocene temperature in the North Atlantic region. Quaternary Research 65, 223–231.

Kawamura, K., Ishiwatari, R., Ogura, K., 1987. Early diagenesis of organic matter in the water column and sediments: microbial degradation and resynthesis of lipids in Lake Haruna. Organic Geochemistry 11, 251–264.

Kenny, R., Markgraf, V., White, J.W.C., 1999. Paleotemperature estimates for the last 14,000 (radiocarbon) years BP from D/H isotopes in peat from Southern South America. Modern Geology 21, 365–378.

Kuder, T., Kruge, M.A., 1998. Preservation of biomolecules in sub-fossil plants from raised peat bogs – a potential paleoenvironmental proxy. Organic Geochemistry 29, 1355–1368.

Lamb, H.F., 2001. Holocene climatic change and vegetation response inferred from the sediments of Ethiopian crater lakes. Proceedings of the Royal Irish Academy 101B, 35–46.

Lamb, H., Roberts, N., Leng, M., Barker, P., Benkaddour, A., van der Kaars, S., 1999. Lake evolution in a semi-arid montane environment: responses to catchment change and hydroclimatic variation. Journal of Palaeolimnology 21, 325–343.

Lamb, A.I., Leng, M.J., Mohammed, M.U., Lamb, H.F., 2004. Holocene climate and vegetation change in the Main Ethiopian Rift Valley, inferred from the composition (C/N and δ^{13}) of lacustrine organic matter. Quaternary Science Reviews 23, 881–891.

Lawrence, R.C., 1966. The metabolism of triglycerides by spores of *Penicilium roqueforti*. Journal of General Microbiology 46, 65–76.

Leahy, J.G., Colwell, R.R., 1990. Microbial degradation of hydrocarbons in the environment. Microbiology Reviews 54, 305–315.

Lehtonen, K., Ketola, M., 1990. Occurrence of long-chain acyclic methyl ketones in Sphagnum and Carex peats of various degress of humification. Organic Geochemistry 15, 275–280.

Lehtonen, K., Ketola, M., 1993. Solvent-extractable lipids of *Sphagnum*, *Carex*, *Bryales*, and *Carex–Bryales* peats: content and compositional features vs. peat humification. Organic Geochemistry 20, 363–380.

Leira, M., 2005. Diatom responses to Holocene environmental changes in a small lake in northwest Spain. Quaternary International 140–141, 90–102.

Magny, M., 1998. Reconstruction of Holocene lake-level changes in the Jura (France): methods and results. In: Harrison, S.P., Frenzel, B., Huckried, U., Weiss, M. (Eds.), Palaeohydrology as Reflected in Lake-level Changes as Climatic Evidence for Holocene Times, Palaoklimaforschung, vol. 25. Akademie der Wissenschaften und Literatur, Mainz, Germany, pp. 67–85.

Magny, M., 2004. Holocene climate variability as reflected by mid-European lake-level fluctuations and its probable impact on prehistoric human settlements. Quaternary International 113, 65–79.

Magny, M., Miramont, C., Sivan, O., 2002. Assessment of climate and anthropogenic factors on Holocene Mediterranean vegetation in Europe on the basis of palaeohydrological records. Palaeogeography, Palaeoclimatology, Palaeoecology 186, 47–59.

Magny, M., Bégeot, C., Guiot, J., Peyron, O., 2003. Contrasting patterns of hydrological changes in Europe in response to Holocene climate cooling phases. Quaternary Science Reviews 22, 1589–1596.

Magny, M., de Beaulieu, J.L., Drescher-Schneider, R., Vannière, B., Walter-Simonnet, A.V., Miras, Y., Millet, L., Bossuet, G., Peyron, O., Brugiapaglia, E., Leroux, A., 2007. Holocene climate changes in the central Mediterranean as recorded by lake-level fluctuations at Lake Accesa (Tuscany, Italy). Quaternary Science Reviews 26, 1736–1758.

Martín Vide, J., Olcina Cantos, J., 2001. Climas y Tiempos de España. Historia y Geografía. Alianza Editorial, Madrid.

Martínez Cortizas, A., Pontevedra-Pombal, X., García-Rodeja, E., Nóvoa-Muñoz, J.C., Shotyk, W., 1999. Mercury in a Spanish peat bog: archive of climate change and atmospheric metal deposition. Science 284, 939–942.

Martínez Cortizas, A., Costa-Casais, M., López-Sáez, J.A., 2009. Environmental change in NW Iberia between 7000 and 500 cal. BC. Quaternary International 200, 77–89.

Martínez García, E., 1980. Mapa Geológico de España 1:50.000, hoja No. 32 (Llanes). IGME, Madrid.

Martín-Puertas, C., Valero-Garcés, B.L., Mata, M.P., González-Sampériz, P., Bao, R., Moreno, A., Stefanova, V., 2008. Arid and humid phases in Southern Spain during the last 4000 years: the Zóñar Lake record, Córdoba. The Holocene 18, 1–15.

Mary, G., de Beaulieu, J.L., Médus, J., 1973. Un diagramme sporopollinique et des datations ^{14}C pour la tourbière du Llano Ronanzas (Asturies-Espagne). Bulletin de la Société Géologique de France supplément XV, 37–38.

Mayewski, P.A., Rohling, E.E., Stager, J.C., Karlen, W., Maasch, K.A., Meeker, L.D., Meyerson, E.A., Gasse, F., van Kreveld, S., Holmgren, K., Lee-Thorp, J., Rosqvist, G., Rack, F., Staubwasser, M., Schneider, R.R., Steig, E.J., 2004. Holocene climate variability. Quaternary Research 62, 243–255.

Mayewski, P.A., Meredith, M.P., Summerhayes, C.P., Turner, J., Worby, A., Barrett, P.J., Casassa, G., Bertler, N.A.N., Bracegirdle, T., Naveira Garabato, A.C., Bromwich, D., Campbell, H., Hamilton, G.H., Lyons, W.B., Maasch, K.A., Aoki, S., Xiao, C., 2009. State of the Antarctic and Southern Ocean climate system. Reviews of Geophysics, 47. doi:10.1029/2007RG000231.

McClymont, E.L., Avsejs, L.A., Nott, C.J., Roberts, Z.E., Volders, F.D.M., Pancost, R.D., Evershed, R.P., 2005. Reconstructing abrupt climate changes over the European land mass during the late Holocene using biomarker analysis of ombrotrophic peats. Abstract. 22nd International Meeting on Organic Geochemistry, Seville, pp. 173–174.

Ménot, G., Burns, S.J., 2001. Carbon isotopes in ombrogenic peat bog plants as climatic indicators: calibration from an altitudinal transect in Switzerland. Organic Geochemistry 32, 233–245.

Meyers, P.A., 2003. Applications of organic geochemistry to paleolimnological reconstructions: a summary of examples from the Laurentian Great Lakes. Organic Geochemistry 34, 261–289.

Meyers, P.A., Ishiwatari, R., 1993. Lacustrine organic geochemistry-an overview of indicators of organic matter sources and diagenesis in lake sediments. Organic Geochemistry 20, 867–900.

Meyers, P.A., Lallier-Verges, E., 1999. Lacustrine sedimentary organic matter records of Late Quaternary paleoclimates. Journal of Paleolimnology 21, 345–372.

Morellón, M., Blas Valero-Garcés, B., Moreno, A., González-Sampériz, P., Mata, P., Romero, O., Maestro, M., Navas, A., 2008. Holocene palaeohydrology and climate variability in northeastern Spain: the sedimentary record of Lake Estanya (Pre-Pyrenean range). Quaternary International 181, 15–31.

Morrison, R.I., Bick, W., 1966. Long-chain methyl ketones in soils. Chemistry and Industry 14, 596–597.

Morrison, R.I., Bick, W., 1967. The wax fraction of soils: separation and determination of some components. Journal of the Science of Food and Agriculture 18, 351–355.

Muller, R.A., MacDonald, G.J., 2000. Ice ages and Astronomical Causes, Data, Spectral Analysis, Mechanisms. Springer Praxis, Chichester.

Muñoz Sobrino, C., 2001. Cambio climático y dinámica del paisaje en las montañas del Noroeste de la Península Ibérica. Ph.D. Thesis. University of Santiago de Compostela, Spain.

Nichols, J.E., Huang, Y., 2007. C_{23}–C_{31} *n*-alkan-2-ones are biomarkers for the genus *Sphagnum* in freshwater peatlands. Organic Geochemistry 38, 1972–1976.

Nichols, J.E., Booth, R.K., Jackson, S.T., Pendall, E.G., Hung, Y., 2006. Paleohydrologic reconstruction based on *n*-alkane distributions in ombotrophic peat. Organic Geochemistry 37, 1505–1513.

Nott, C.J., Xie, S., Avsejs, L.A., Maddy, D., Chambers, F.M., Evershed, R.P., 2000. *n*-Alkane distribution in ombotrophic mires as indicators of vegetation change related to climatic variation. Organic Geochemistry 31, 231–235.

Ogura, K., Machilara, T., Takada, H., 1990. Diagenesis of biomarkers in Biwa lake sediments over 1 million years. Organic Geochemistry 16, 805–813.

Ortiz, J.E., Torres, T., Delgado, A., Julià, R., Lucini, M., Llamas, F.J., Reyes, E., Soler, V., Valle, M., 2004. The palaeoenvironmental and palaeohydrological evolution of Padul Peat bog (Granada, Spain) over one million years, from elemental, isotopic and molecular organic geochemical proxies. Organic Geochemistry 35, 1243–1260.

Pancost, R.D., Baas, M., van Geel, B., Sinninghe Damsté, J.S., 2002. Biomarkers as proxies for plant inputs to peats: an example from a sub-boreal ombotrophic bog. Organic Geochemistry 33, 675–690.

Peña-Chocarro, L., Zapata, L., Iriarte, M.J., González Morales, M., Straus, L., 2005. The oldest agriculture in Northern Atlantic Spain. Journal of Archaeological Science 32, 579–587.

Peñalba, M.C., 1989. Dynamique de vegetation Tardiglaciaire et Holocene du Centre-Nord de l'Espagne d'aprés l'analyse pollinique. Ph.D. Thesis, Université d'Aix-Marseille III, France.

Pons, A., Reille, M., 1988. The Holocene and upper Pleistocene pollen record from Padul (Granada, Spain): a new study. Palaeogeography, Palaeoclimatology, Palaeoecology 66, 243–263.

Reed, J.M., Stevenson, A.C., Juggins, S., 2001. A multi-proxy record of Holocene climatic change in southwestern Spain: the Laguna de Medina, Cadiz. Holocene 11, 707–719.

Rieley, G., Collier, R.J., Jones, D.M., Eglinton, G., 1991. The biogeochemistry of Ellesmere Lake, UK – I: source correlation of leaf wax inputs to the sedimentary record. Organic Geochemistry 17, 901–912.

Riera, R., Wansard, G., Julià, R., 2004. 2000-year environmental history of a karstic lake in the Mediterranean Pre-Pyrenees: the Estanya lakes (Spain). Catena 55, 293–324.

Riera-Mora, S., Esteban-Amat, A., 1994. Vegetation history and human activity during the last 6000 years on the central Catalan coast (northeastern Iberian Peninsula). Vegetation History and Archaeobotany 3, 7–23.

Rivas-Martínez, S., Rivas y Sáenz, S., 2006. Worldwide Bioclimatic Classification System. <http://www.globalbioclimatics.org> (15.01.06).

Roberts, N., Lamb, H.F., El Hamonti, N., Barker, P., 1994. Abrupt Holocene hydroclimatic events palaeolimnological evidence from North-west Africa. In: Millington, A.C., Pye, K. (Eds.), Environmental Change in Drylands: Biogeographical and Geomorphological Perspectives. Wiley, Chichester, pp. 163–175.

Roca, J.R., Julià, R., 1997. Late-glacial and Holocene lacustrine evolution based on ostracode assemblages in Southeastern Spain. Geobios 30, 823–830.

Salas, L., 1992. Propuesta de modelo climático para el Holoceno en la vertiente cantábrica en base a los datos polínicos. Cuaternario y Geomorfología 6, 63–69.

Schilman, B., Bar-Matthews, M., Almogi-Labin, A., Luz, B., 2001. Global climate instability reflected by Eastern Mediterranean marine records during the late Holocene. Palaeogeography, Palaeoclimatology, Palaeoecology 176, 157–176.

Stuiver, M., Reimer, P.J., 1993. Extended ^{14}C database and revised CALIB radiocarbon calibration program. Radiocarbon 35, 215–230.

Stuiver, M., Reimer, P.J., Reimer, R.W., 2005. Calib Radiocarbon Calibration Version 5.0: Copyright 1986–2005. <http://calib.qub.ac.uk/calib/> (31.01.09).

Valero Garcés, B., Moreno, A., Navas, A., Mata, P., Machín, J., Delgado Huertas, A., González Sampériz, P., Schwalb, A., Morellón, M., Cheng, H., Edwards, R.L., 2008. The Taravilla lake and tufa deposits (Central Iberian Range, Spain) as palaeohydrological and palaeoclimatic indicators. Palaeogeography, Palaeoclimatology, Palaeoecology 259, 136–156.

Van der Knaap, W.O., Van Leeuwen, J.F.N., 1995. Holocene vegetation succession and degradation as responses to climatic change and human activity in the Serra da Estrela, Portugal. Review of Palaeobotany and Palynology 89, 153–211.

Vegas, J., 2007. Caracterización de eventos climáticos del Pleistoceno superior-Holoceno mediante el estudio sedimentológico de la Laguna Grande (Sierra Neila, NO Sistema Ibérico). Revista de la Sociedad Geológica de España 20, 53–70.

Verschuren, D., Lalrd, K.R., Cumming, B.F., 2000. Rainfall and drought in equatorial east Africa during the past 1100 years. Nature 403, 410–414.

Viso, A.C., Pesando, D., Bernard, P., Marty, J.C., 1993. Lipids components of the Mediterranean seagrass Posidonea Oceanica. Phytochemistry 34, 381–387.

Volkman, J.K., Smith, D.J., Eglinton, G., Forsberg, T.E.V., Corner, E.D.S., 1981. Sterol and fatty acid composition of four marine Haptophycean algae. Journal of the Marine Biological Association 61, 509–527.

White, J.W.C., Ciais, P., Figge, R.A., Kenny, R., Markgraf, V., 1994. A high resolution record of atmospheric CO_2 content from carbon isotopes in peat. Nature 367, 153–156.

Xie, S., Nott, C.J., Avsejs, L.A., Maddy, D., Chambers, F.M., Evershed, R.P., 2004. Molecular and isotopic stratigraphy in an ombotrophic mire for paleoclimate reconstruction. Geochimica et Cosmochimica Acta 68, 2849–2862.

Zheng, Y., Zhou, W., Meyers, P.A., Xie, S., 2007. Lipid biomarkers in the Zoigê-Hongyuan peat deposit: indicators of Holocene climate changes in West China. Organic Geochemistry 38, 1927–1940.

Zhou, W., Xie, S., Meyers, P.A., Zheng, Y., 2005. Reconstruction of late glacial and Holocene climate evolution in southern China form geolipids and pollen in the Dingnan peat sequence. Organic Geochemistry 36, 1272–1284.